INDIAN JOURNAL OF SCIENCE AND TECHNOLOGY

ORIGINAL ARTICLE

Check for updates

OPEN ACCESS

Received: 30/04/2025

Accepted: 18/07/2025

Published: 20/08/2025

Citation: Kumari S, Prasad S, Chandel S (2025) The Chemical Reaction Effect on MHD Viscoelastic Nanofluids Flow over a Stretching Sheet Embedded in Porous Media with Thermal Radiation. Indian Journal of Science and Technology 18(31): 2539-2554. https://doi.org/10.17485/IJST/v18i31.816

* **Corresponding author**.

Funding: None

Competing Interests: None

Published By Indian Society for Education and Environment (iSee)

ISSN
Print: 0974-6846
Electronic: 0974-5645

The Chemical Reaction Effect on MHD Viscoelastic Nanofluids Flow over a Stretching Sheet Embedded in Porous Media with Thermal Radiation

S Kumari[1], **S Prasad**[2], **S Chandel**[3]*

1 Research scholar, Mathematics and statistics, Career Point University, Hamirpur, India
2 Assistant professor, School of Basic Sciences, Abhilashi University, Mandi, India
3 Assistant professor, Mathematics and statistics, Career Point University, Hamirpur, India

Abstract

Objective: In the current study, we investigate the impact of chemical Reaction effect on MHD viscoelastic nanofluids flow over a stretching sheet embedded in porous media with thermal radiation. **Methods:** The governing partial differential equations describing the flow were converted into a system of non-linear ordinary differential equations through the application of similarity transformation. This system of non-linear equations is addressed using an effective numerical method known as the bvp4c method. The influences of the thermal radiation parameter, chemical reaction parameter, heat source parameter, thermophoresis parameter, and Brownian motion parameter on various flow characteristics, Lewis number, porosity parameter, magnetic field parameter, temperature, concentration, skin friction coefficient, Nusselt number, and Sherwood number, are graphically presented and thoroughly discussed. **Findings:** Graphical representations of velocity, temperature and concentration distributions reveal the influence of emerging flow variables. Velocity distributions $f'(\eta)$ rises for increasing values of viscoelastic parameter, magnetic parameter, Darcy- Forchheimer and while declines for porosity parameter. In concentration profile $\phi(\eta)$ boosts for higher values of Darcy-Forchheimer parameter, magnetic parameter and declines for viscoelastic parameter, porosity parameter. In temperature profile $\theta(\eta)$ boosts for higher values of Darcy- Forchheimer parameter, and declines for porosity parameter, viscoelastic parameter. **Novelty:** This topic explores the novel intersection of MHD, viscoelastic nanofluids, porous media, thermal radiation, and chemical reaction. The combination of these factors is comparatively unexplored, providing opportunities for new insights. The study's findings could have implications for advanced heat transfer enhancement, energy systems, and biomedical applications. It contributes to advancing the understanding of complex fluid dynamics and thermodynamics.

Keywords: Thermal radiation; Chemical reaction MHD; Heat and mass transfer; Stretching surface; Porous medium

1 Introduction

The stretching of sheets during manufacturing process has a profound effect on the quality of end product. The flow generated by an extending surface contains significant importance in various industrial and technical applications. Materials manufactured through various processes, such as polymer extrusion and gem development, paper production, glass fiber manufacturing, wire drawing and hot rolling, plastic film extrusion, tempering and timing of copper wires, cooling of electronic chips or metallic sheets. These industrial applications rely heavily on the flow caused by extending surfaces, highlighting its significance in modern manufacturing processes. In all these cases, the final product's desirable properties are determined by the rate at which it is stretched and cooled. Mohammed[1] study convective heating and slip velocity effects on viscoelastic nanofluid and heat transfer over stretching sheets. Mat Noor et al. and S. Hosseinzadeh et al.[2]-[3] observed the Walters'-B fluid display viscoelastic properties, showcasing both viscosity and elasticity. Nanofluids have emerged as a promising area of research, attracting attention from scientists and engineers globally, owing to their capacity to improve the thermal conductivity of traditional fluids, such as water, oils, and ethylene glycol, and improve heat transfer characteristics. The term nanofluids is a type of a liquid that contains nanoparticles, which can be composed of metal or non- metal materials and have dimensions of 100 nanometers or smaller. Nanofluids offer a wide range of applications, from enhancing cooling systems in nuclear reactors and industrial settings, to improving automotive and avionics systems, and even contributing to advancements in medical treatments, such as cancer therapy and antimicrobial therapies. By utilizing nanofluids as coolants, radiators could be designed to be smaller and more compact, allowing for more effective placement and reduced spatial requirements. Nanofluids offer significant advantages in solar energy absorption systems, where they can absorb energy directly and reduce reliance on intermediate heat transfer mechanisms. Optimizing the size and shape of nanoparticles for particular uses can significantly boost absorption capabilities, resulting in better overall performance. The study of fluid fluxes and transport phenomena in porous spaces with high Reynolds numbers is crucial, with significant applications in pharmaceutical, chemicals, food processing and ecology. Many environmental and industrial systems, including geothermal energy and heat exchanger design systems, rely on convective flow through permeable media. As a result, Numerous researchers, including Shahin et al.[4], Mohammed[5], and Elham et al.[6] have explored nanofluids under various flow condition due to their substantial practical importance and widespread presence in multiple scientific and engineering disciplines. A wide range of technological applications, such as geothermal energy systems, catalytic reactors, and waste management, have fueled significant research interest in heat transfer and nanofluid dynamics within porous materials. The significance of this topic has led to an excess of studies examining fluid flow through porous media NS. Yousef et al.[7] explored chemical reaction impact on MHD dissipative flow of Casson Williamson nanofluid over a porous stretching sheet with slip effects. In various practical applications, mass transfer occurs through diffusive processes, involving molecular diffusion of species, often accompanied by homogeneous and heterogeneous chemical reactions. Homogeneous reactions exhibit uniform heat generation throughout a phase, whereas heterogeneous reactions are localized, occurring within a specific region or at the interface between phases. A fundamental of first order chemical reactions is that the reaction rate is directly proportional to the concentration of the reacting species. The diffusive species can undergo various chemical reactions with the surrounding fluid, leading to absorption or generation, which significantly impacts the properties and quality of the final products. Crane's study expanded on Sakaidis' research on flow induced by a moving surface, focusing specifically on the flow behavior caused by a linearly stretching sheet. Rahimah et al.[8] explored the thermal radiation effect on Viscoelastic Walters'-B nanofluid flow through a circular cylinder in convective and constant heat flux. Zhi-Min et al.[9] investigated that Impact of porous and magnetic dissipation on dissipative fluid flow and heat transfer in the presence of darcy-brinkman porous medium. Kavitha et al.[10] studied the Numerical Investigation on Heat and Mass transfer through a porous medium in the presence of MHD and Chemical Reaction. Parakapali et al.[11] investigated Radiative MHD Flow of a Micropolar Nanofluid past stretching/shrinking sheets with heat generation/Absorption. Salisu et al.[12] explored that the Magneto hydrodynamic (MHD) Convective Flow through a Porous Medium with Magnetic and Chemical Reaction Characteristics. Shandhya et al.[13] studied heat and mass transfer effects on MHD flow past an inclined porous plate in the presence of chemical reaction [International Journal of Applied Mechanics and Engineering]. Jothimani[14] investigated that the Unsteady Casson fluids flow past a stretching sheet with radiation absorption and chemical reaction. Hosseinzadeh et al.[15] explored the Hydrothermal analysis on non-Newtonian nanofluid flow of blood through porous vessels. Safyan[16] analyzed that the thermal radiation and mixed convection effects on MDH viscoelastic nanofluid flow past an elongated surface. D. Hymavathi[17] explored the micropolar Nanofluid Flow, Thermal and Mass Transfer Properties Across a Stretching Sheet with a Predetermined Surface Heat Flux. Vinodkumar et al.[18] studied the impact of hall current and thermal radiation on mixed convection flow of Ree- Eyring nanofluid with bioconvection. Devika et al.[19] explored nanoparticle shape and thermal radiation effects on Viscoelastic nanofluid flow in porous channels with MHD. Muhammad shoaib et al.[20] emphasizes the investigation of heat transfer characteristics in MHD hybrid nanofluids, focusing on the effects of variable viscosity and thermal radiation. Waheed abdelwahab et al.[21] studied chemical reaction impact on MHD nanofluid flow with temperature- dependent viscosity on heat and mass transfer.

Limited studies have focused on viscoelastic fluid behavior over stretching sheets, highlighting a gap in current knowledge. No existing studies have investigated the interplay between variable conductivity and convective heating in viscoelastic nanofluid dynamics. This study addresses existing research gaps by exploring convective heating and heat transfer in dissipative Viscoelastic fluid flow over a permeable, slippery stretching sheet within a porous medium, considering thermal radiation effects.

2 Methodology

Consider the two dimensional steady MHD flow of viscoelastic nanofluids past a non-conducting stretching surface y = 0 embedded in a porous medium, taking into account the impact of internal heat generation, thermal radiation, and chemical reactions. The melting stretching sheet, positioned at y = 0, exhibits specific velocity, temperature, and concentration distributions that affect the flow behavior u = Uw(x), T = Tm, and C = Cw respectively. A schematic representation of the flow configuration, including the coordinate system, is shown in Figure 1.

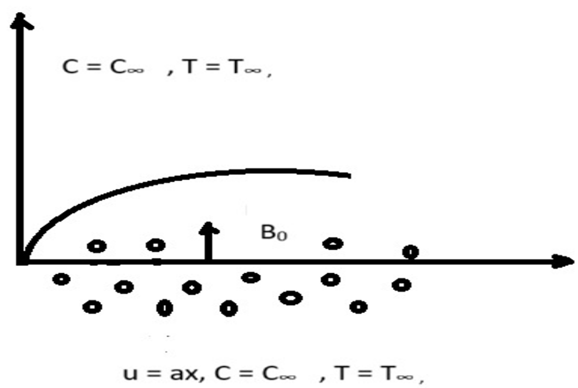

Fig 1. Flow configuration

The primary goal of this research is to investigate the impact of nanoparticles on the two dimensional boundary layer flow of a viscous fluid.

The governing equation for the nanofluid in Cartesian coordinates following Rashidi et al,[22] with boundary conditions is given by

$$\frac{\partial u}{\partial x}+\frac{\partial v}{\partial y}=0 \tag{1}$$

$$u\frac{\partial u}{\partial x}+v\frac{\partial u}{\partial y}=\nu\frac{\partial^2 u}{\partial y^2}+\frac{k}{\rho}\left[u\frac{\partial^3 u}{\partial u\,\partial y^2}+v\frac{\partial^3 u}{\partial y^3}+\frac{\partial u}{\partial x}\frac{\partial^2 u}{\partial y^2}-\frac{\partial u}{\partial y}\frac{\partial^2 u}{\partial x\,\partial y}\right]-\sigma\frac{B_0^2 u}{\rho}-\frac{\mu}{\rho}u-Fu^2 \tag{2}$$

$$u\frac{\partial T}{\partial x}+v\frac{\partial T}{\partial y}=\nu\frac{\partial^2 T}{\partial y^2}+\tau[D_B\frac{\partial C}{\partial y}\frac{\partial T}{\partial y}+\frac{D_T}{T_\infty}\left(\frac{\partial T}{\partial y}\right)^2-\frac{\partial q_r}{\partial y}+\frac{Q}{\rho c_p}(T-T_\infty) \tag{3}$$

$$u\frac{\partial C}{\partial x}+v\frac{\partial C}{\partial y}=D_B\frac{\partial^2 C}{\partial y^2}+\frac{D_T}{T_\infty}\frac{\partial^2 T}{\partial y^2}-k_c(C-C_W) \tag{4}$$

The boundary conditions for the flow analysis are specified as

$$u=u_w(x)=ax, v=0, T=T_{W,}\ C=C_W\ \ at\ y=0,$$

$$k\left(\frac{\partial T}{\partial y}\right)\rho\left[\beta+c_s\left(T_W-T_\infty\right)\right]v\left(x,0\right) \tag{5}$$

$$u\to 0,\ T\to T_\infty,\ C\to C_\infty\ \ as\ y\to\infty \tag{6}$$

Where u and v are the velocity components in the x and y directions, v the kinematic viscosity, $\tau=(\rho c)_p/(\rho c)_f$ is the ratio of nanoparticles heat capacity and the base fluid heat capacity, D_B is the Brownian diffusion coefficient, D_T is the thermophoretic diffusion coefficient, T_∞ ,C_∞ are the reference temperature and reference concentration, respectively. The radioactive flux is accounted by employing the Rossland assumption in the energy equation.

$$q_r=-\frac{4\sigma}{3kk^*}\frac{\partial T^4}{\partial y} \tag{7}$$

in which σ the Stefan- Boltzmann constant and k the mean absorption coefficient. Further, the differences of temperature within the flow is assumed to be small such that T^4 may be expressed as a linear function of temperature. Expanding T^4 about. T_∞ by Taylors series and ignoring higher order terms, we have

$$T^4={T^4}_\infty+T-T_\infty 4{T^3}_\infty=4{T^3}_\infty T-3{T^4}_\infty \tag{8}$$

By employing **equation (7)** and **equation (8)**, **equation (3)** has the form

$$u\frac{\partial T}{\partial x}+v\frac{\partial T}{\partial y}=\nu\frac{\partial^2 T}{\partial y^2}+\tau[D_B\frac{\partial C}{\partial y}\frac{\partial T}{\partial y}+\frac{D_T}{T_\infty}\left(\frac{\partial T}{\partial y}\right)^2+\frac{Q}{\rho c_p}\left(T-T_\infty\right)+\frac{16\sigma}{3k}\frac{\partial T^3}{\partial y} \tag{9}$$

The **equations (2)-(6) and (9)** can be reduced into the dimensionless form by introducing the following new variables (20).

$$u=axf'(\eta),\ v=-\sqrt{cv}f(\eta),\ \theta(\eta)=\frac{T-T_\infty}{T_W-T_\infty},\phi(\eta)=\frac{C-C_W}{C_W-C_\infty},\eta=y\sqrt{\frac{c}{v}} \tag{10}$$

Where η represents the dimensionless similarity variable, v denotes the non-dimensional stream function, θ represents the non-dimensional fluid temperature and ϕ denotes the dimensionless concentration. The nanofluids's viscosity and thermal conductivity are considered to vary with dimensionless temperature θ, whereas the Brownian diffusion coefficient varies t dimensionless concentration ϕ.

The above transformations satisfy **equation (1)** identically. The equations of linear momentum energy and concentration in dimensionless form become

$$f'''+ff''-f'^2-Rc\left[2f'f'''-ff^{iv}-f'^2\right]-(M+A)f'+Fr\,f'^2=0 \tag{11}$$

$$(1+Rd)\theta''+Pr(f'\theta+Q\theta+Nb\,\theta'\phi'+Nt\,\theta'^2=0 \tag{12}$$

$$\phi''+PrLef\phi'+\frac{Nt}{Nb}\theta''-\Pr Le\,Sf'=0 \tag{13}$$

Along with the following specified boundary constraints

$$f=b,\quad f'=1,\quad \phi=1,\quad \theta'=0,\quad at\ \eta\to 0$$

$$f'\to 0,\quad f''\to 0,\quad \theta\to 0,\quad \phi\to 0,\quad at\ \eta\to\infty \tag{14}$$

It is evident that the Magnetic field M, Lewis number Le, Porosity parameter A, Viscoelastic parameter Rc, Suction parameter b, Chemical reaction S, Darcy- Forchheimer Fr, Thermal radiation Rd, Prandtl number Pr, Brownian motion parameter Nb, Thermophoresis parameter Nt, each of which can be specified as follows, affect the momentum equation.

$$\begin{gathered} M=\frac{\sigma B_0^2}{\rho\nu},\ Le=\frac{\alpha}{D_B},\ A=\frac{Aa}{\nu},\ Rc=\frac{ka}{\rho v},\ b=\frac{\nu}{\sqrt{a}}\ \ S=\frac{k_c}{\rho},\ Fr=Fr, \\ Rd=\frac{16\sigma}{3k}\frac{\partial T^3}{\partial y},\ Pr=\frac{v}{\alpha},Nb=\frac{\tau D_B\left(C_W-C_\infty\ \right)}{\nu},\ Nt=\frac{\tau D_T\left(T_W-T_\infty\right)}{\nu T_\infty}, \end{gathered} \tag{15}$$

The shearing stress, surface heat flux and surface mass flux are given by

$$\tau_w=\mu\left(\frac{\partial u}{\partial y}\right)_{y=0}-k\left(u\frac{\partial^2 u}{\partial x\partial y}+v\frac{\partial^2 u}{\partial y^2}+\frac{\partial u}{\partial x}\frac{\partial u}{\partial y}\right),-q_w=\left(\frac{\partial T}{\partial y}\right)_{y=0},\ q_m=D_B\left(\frac{\partial C}{\partial y}\right)_{y=0} \tag{16}$$

The non-dimensional shear stress coefficient $C_f=\tau_{\frac{w}{\rho U^2{}_w}}$, local Nusselt number $Nu_x\ \frac{xq_w}{k\ (T_\infty-T_m)}$, and local Sherwood number $Sh_x=\ \frac{xq_m}{k\ (C_\infty-C_w)}$ are given by

$$\begin{gathered} C_f\left(Re_x\right)^{\frac{1}{2}}=-\left(1-Rc\right)f'(0)\right)f''(0) \\ Nu_x\ \left(Re_x\right)^{\frac{1}{2}}=-\theta'(0) \\ Sh_x\left(Re_x\right)^{\frac{1}{2}}=-\phi'(0) \end{gathered} \tag{17}$$

Where $Re_x=\frac{ax^2}{\nu}$ is the local Reynolds number

2.1 NumericalTechnique:bvp4csolver

The solution of the partial differential **Equation (2), Equation (3) and Equation (4)** is obtained by reducing them to nonlinear ordinary differential **equation (11), Equation (12) and Equation (13)** and solving these equations using MATLAB's bvp4c boundary value problem solver. The complexity of the equations is reduced by introducing dimensionless variables, enabling a more straight forward solution. The ordinary differential equations are optimized for numerical solution by simplifying their mathematical structure. The implementation details of the bvp4c solver for current problem will be discussed in the subsequent section. The initial two steps focusing on simplifying the system of ordinary differential equations, resulting in a reduced form consisting of five first order equations. The boundary conditions are implementation in step 1, and step 4 involves completing the program's implementation.

Step 1 : First and foremost , we'll introduce some components for the paired non- linear ordinary differential equations in **Equation (11), Equation (12) and Equation (13)**. Firstly, we introduce our system of equation by new variables.

$$\begin{gathered} f(0)=y(1),\quad f'(0)=y(2),\quad f''(0)=y(3),\quad f'''(0)=y(4), \\ \theta(0)=y(5),\quad \theta'(0)=y(6),\quad \phi(0)=y(7),\quad \theta'(0)=y(8) \end{gathered} \tag{18}$$

Step 2: Now, in the first order system of equations, we will write these new components as follows:

$$f'=y(2),\quad f''=y(3)$$

$$f^{iv}=\frac{1}{Rc\,y(1)}\left(Rc\left(2\,y(2)y(3)-y(2)^2\right)+(M+A)Y(2)-Fr\,y(2)^2-y(4)-y(1)y(3)+y(2)^2\right) \tag{19}$$

$$\theta=y(5),\quad \theta'=y(6)$$

$$\theta'' = -\left(\frac{1}{1+Rd}\right)(Pr(y(1)y(6) + Qy(5) + Nby(6)y(8) + Nt\, y(6)^2 \tag{20}$$

$$\phi = y(7), \quad \theta' = y(8)$$

$$\phi'' = -(\Pr Le\, y(1)y(8)) + \frac{Nt}{Nb}\left(\frac{1}{1+Rd}\right)(Pr(y(1)y(6) + Qy(5) + Nby(6)y(8) + Nt\, y(6)^2 + \Pr Le\, Sy(7) \tag{21}$$

Step 3: According to the new component, the boundary conditions are expressed as

$$ya(1) - b, \quad ya(2) - 1, \quad ya(6) - 1, \quad ya(7) - 1$$

$$yb(2) \to 0, \quad yb(3) \to 0, \quad yb(5) \to 0, \quad yb(7) \to 0 \tag{22}$$

Table 1. Comparison of – (1-K) f” (0) for different values of K with the result of Rajagopal et al.[23] when A = Fr = S = 0

K	Rajagopal et al.[23]	Present outcome
0.005	-0.9975	-0.9975
0.01	-0.9949	-0.995
0.03	-0.9846	-0.9849
0.05	-0.9738	-0.9748

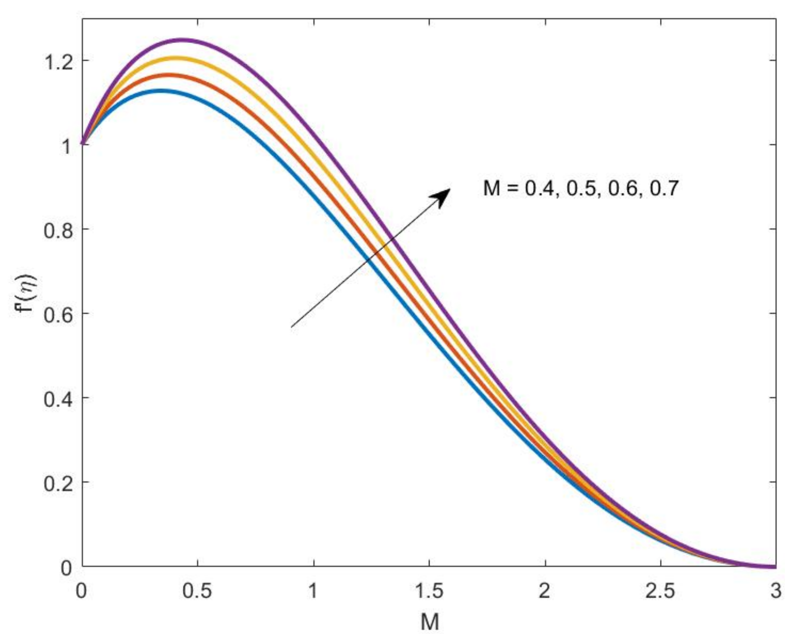

Fig 2. Effect of Magnetic field parameter [M] on the velocity profile $f^{'}(\eta)$

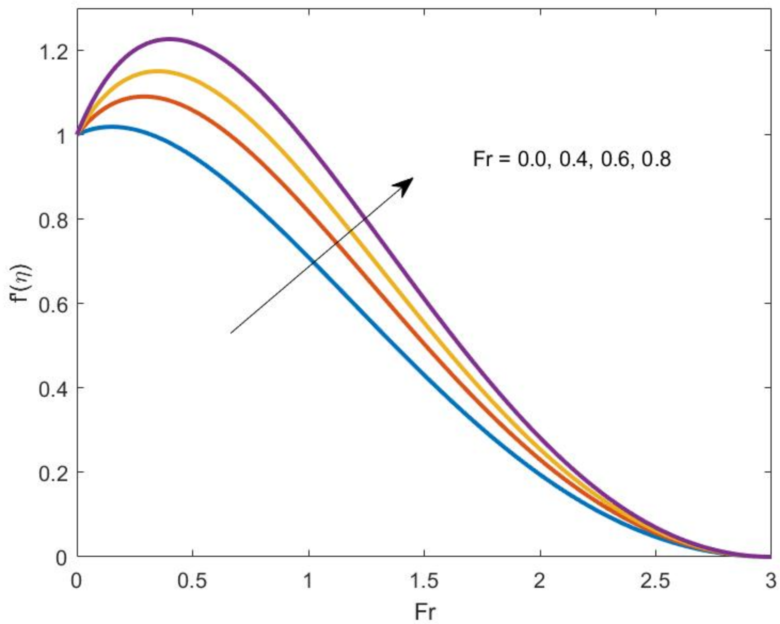

Fig 3. Effect of Darcy Forchheimer [Fr] on the velocity profile $f^{'}(\eta)$

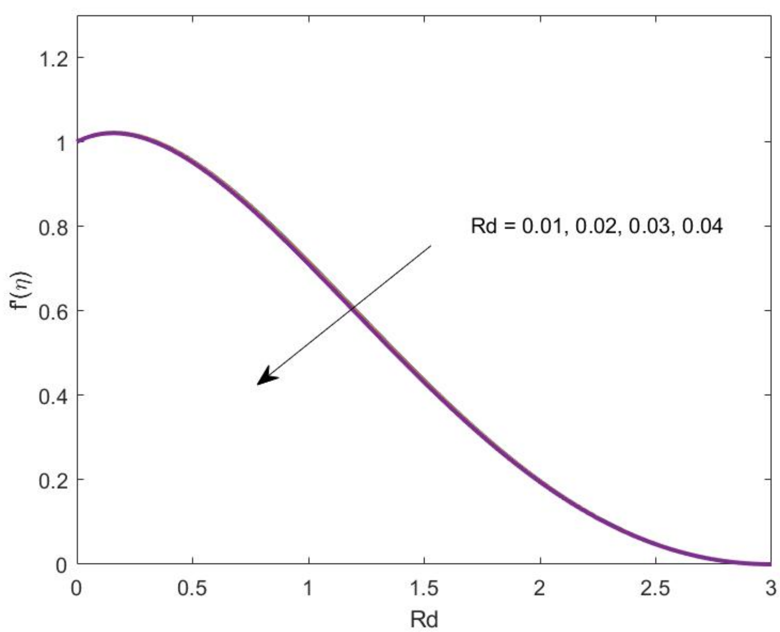

Fig 4. Effect of Thermal radiation parameter [Rd] on the velocity profile $f^{'}(\eta)$

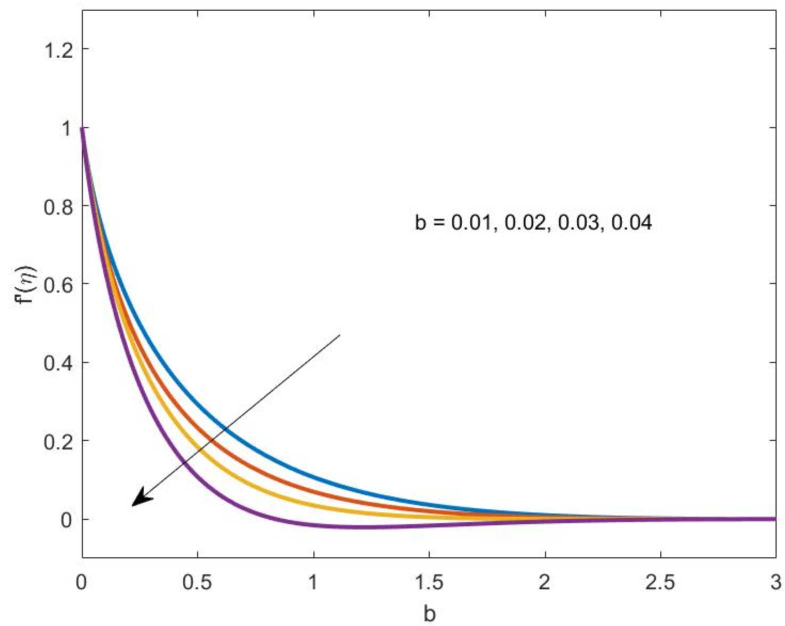

Fig 5. Effect of Suction parameter [b] on the velocity profile $f'(\eta)$

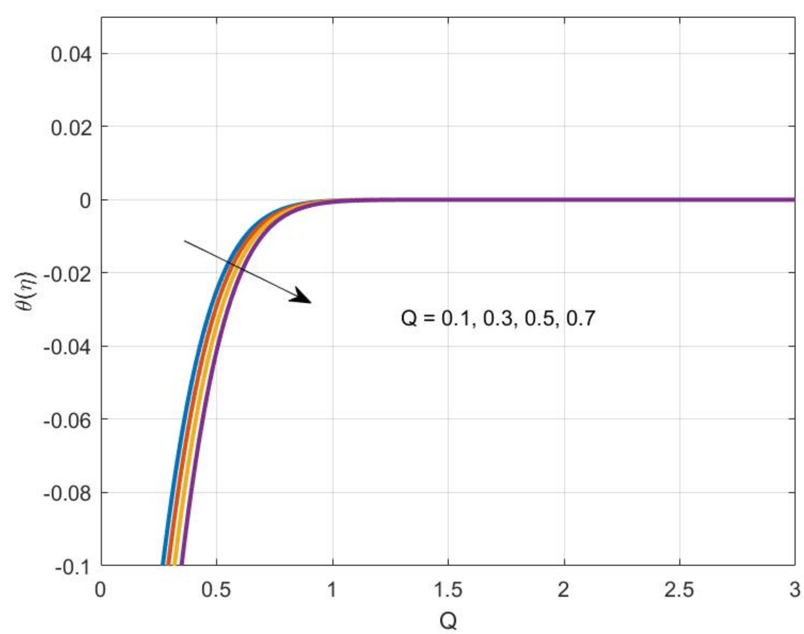

Fig 6. Effect of Heat source parameter [Q] on the temperature profile $\theta(\eta)$

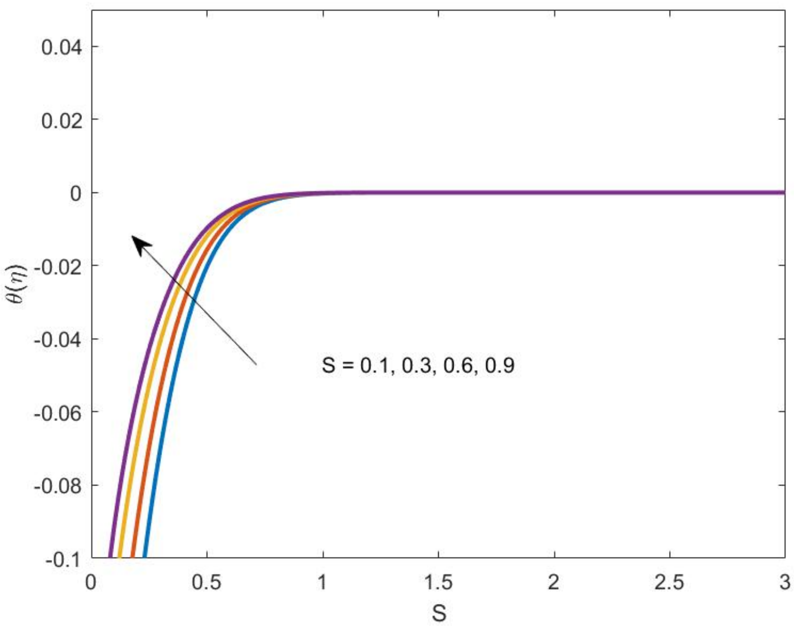

Fig 7. Effect of Chemical reaction parameter [S] on the temperature profile $\theta(\eta)$

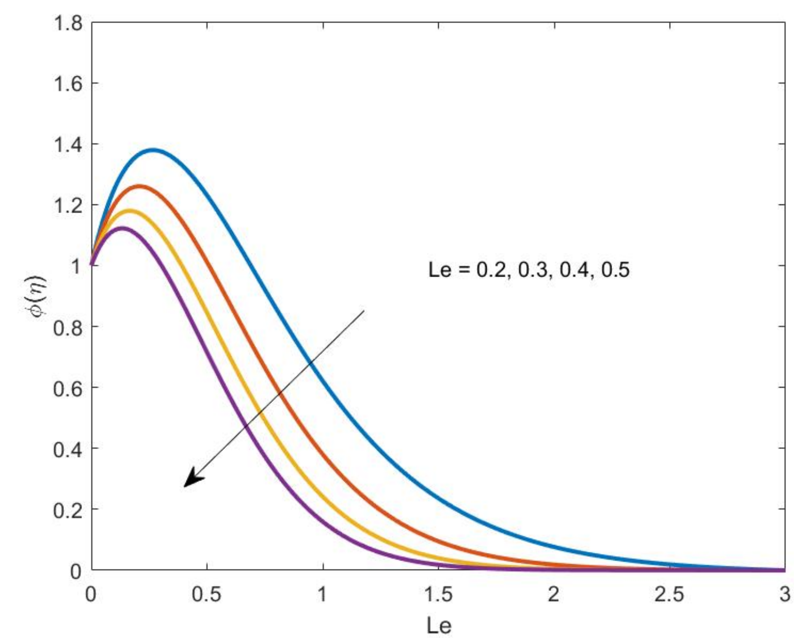

Fig 8. Effect of Lewis number [Le] on Concentration profile $\phi(\eta)$

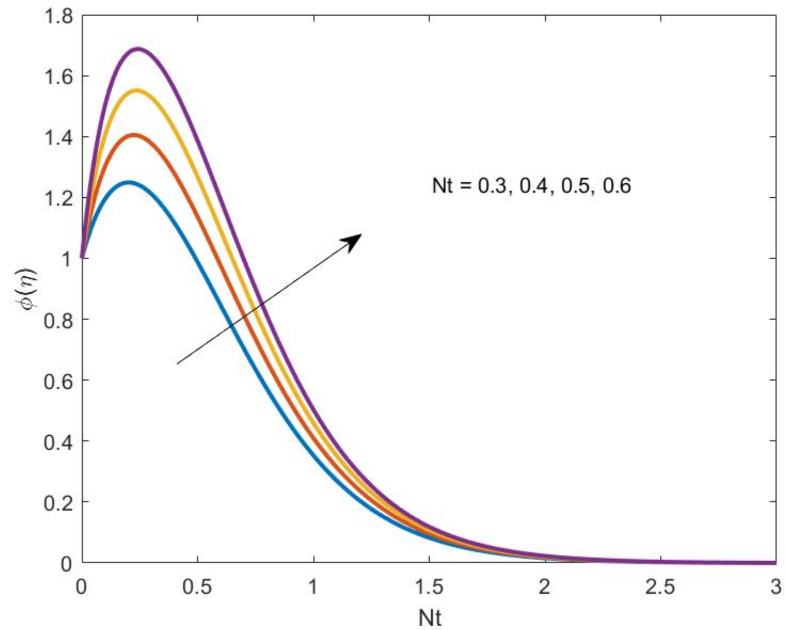

Fig 9. Effect of thermophoresis parameter [Nt]on Concentration profile $\phi(\eta)$

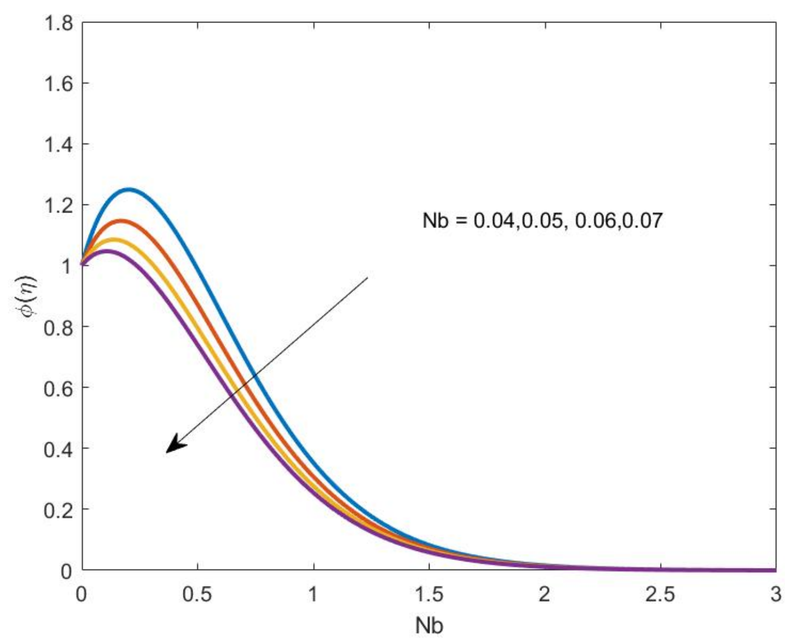

Fig 10. Effect of Brownian motion parameter Nb on Concentration profile $\phi(\eta)$

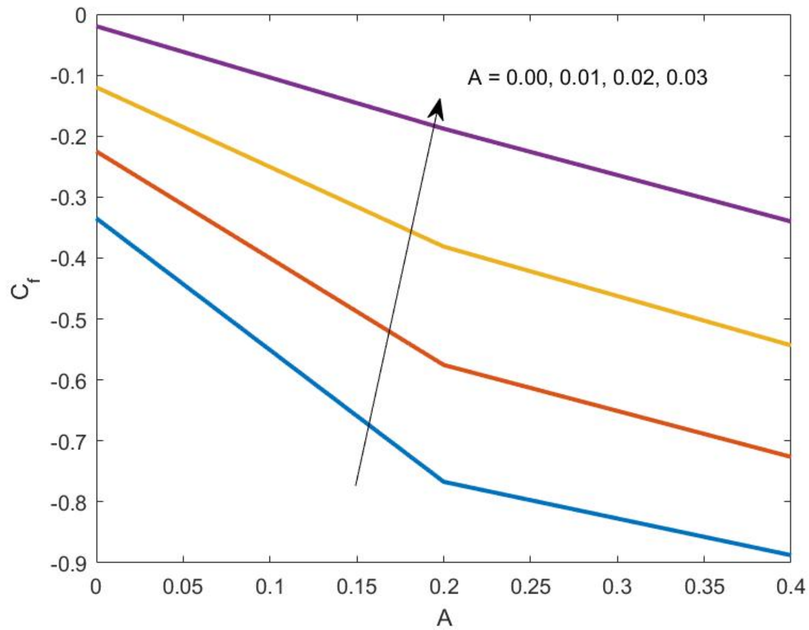

Fig 11. Influence of Porosity parameter [A] on skin friction $[C_f]$ when Pr = 6.2

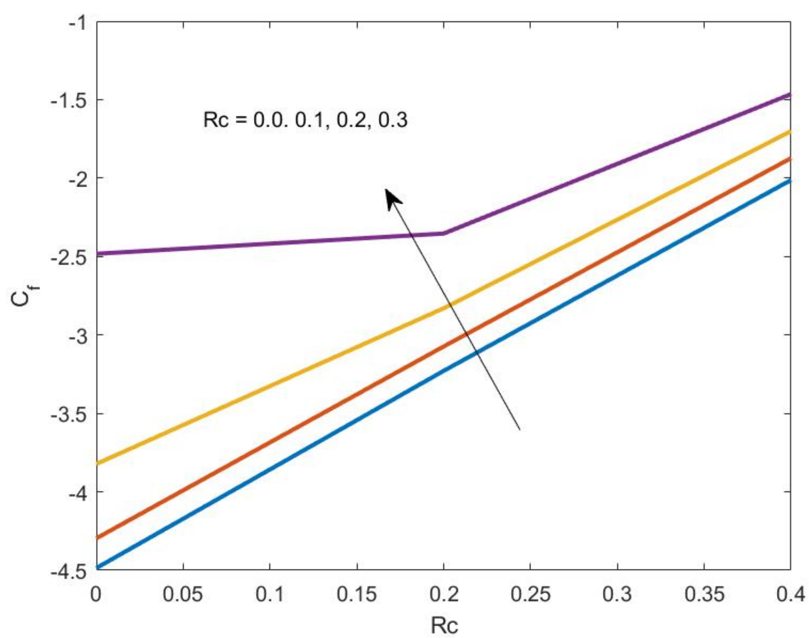

Fig 12. Influence of Viscoelastic coefficient parameter [Rc] on skin friction $[C_f]$ when Pr = 6.2

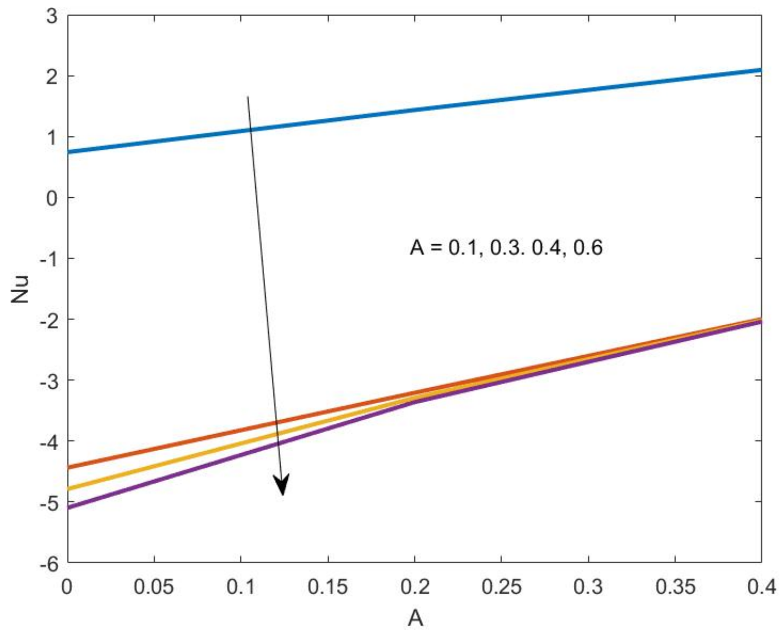

Fig 13. Influence of Porosity parameter [A] on Nusselt number [Nu] when Pr = 6.2

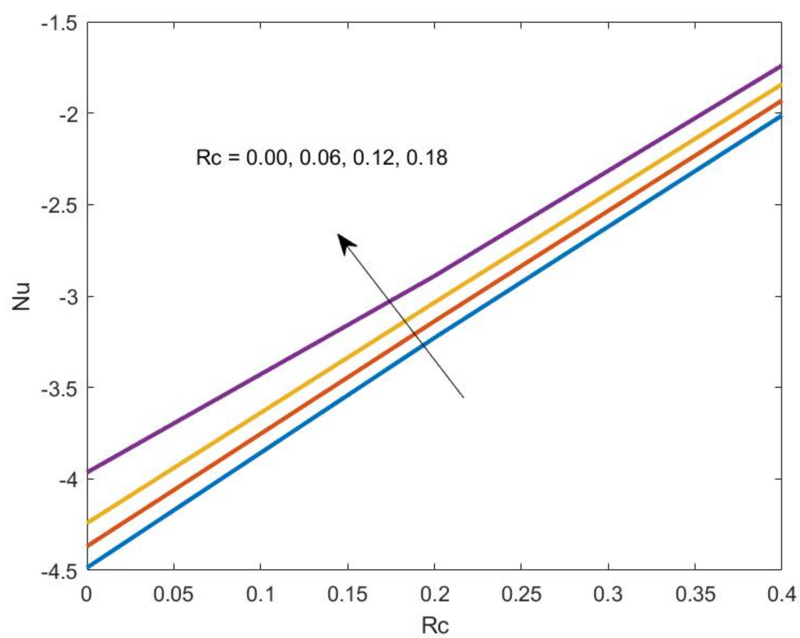

Fig 14. Influence of Viscoelastic coefficient parameter [Rc]on Nusselt number [Nu] when Pr = 6.2

3 Results and Discussion

The local similar solutions of **Equations (11), Equation (12) and Equation (13)** are determined numerically employing the bvp4c method. The scrutinize the influence of different value of Magnetic field parameter M, Porosity parameter A, Prandtl number Pr, Darcy Forchheimer Fr, Lewis number Le, Thermophoresis parameter Nt, Brownian motion parameter Nb, Thermal radiation parameter Rd, Heat source parameter Q, Chemical reaction parameter S, Viscoelastic coefficient parameter Rc, Suction parameter b. The numerical results obtained are utilized to illustrate boundary layer profiles of velocity $f'(\eta)$ and temperature $\theta(\eta)$ in the and concentration profile $\phi(\eta)$ form of figures for various values of the relevant parameters. In this study, the following default numbers are used to do calculations: M = 0.02, A = 0.3, Pr= 6.2, Fr = 0.02, Le = 0.3, Nt = 0.3, Nb = 0.04, Rd = 0.4, Q = 0.01, S = 0.01, Rc = 0.02, b = 0.4. Figure 2 our analysis shows that the magnetic parameters M have a positive effect on the velocity profile, leading to increased velocity and enhance boundary layer thickness. The resistive electromagnetic force, also known as the Lorentz force, opposes the flow in the primary direction, which is a fundamental concept in magneto hydrodynamics. This force arises from the interaction between the magnetic field and the electrically conducting fluid, and it can significantly impact the flow behavior. Figure 3 shows the effects of Darcy- Forchheimer parameter on velocity distribution. We see that the distributions of the nanofluid velocity, is improve because Darcy Forchheimer are excluded, signifying that the sheet is impervious. Therefore, as Darcy- Forchheimer parameter climbs, thermal boundary layer thickness, magnifying cooling behavior. Figure 4 thermal radiation parameter Rd affects the velocity distribution $f'(\eta)$. We observed that as the thermal radiation parameter Rd decreases, the velocity profile and boundary layer thickness also exhibit a decreasing trend. Figure 5 suction parameter b affects the velocity distribution $f'(\eta)$. We see that the distributions of the nanofluid velocity, is decline because suction parameter included in indicating that the sheet is permeable. Therefore, as the suction parameter decreases, the thermal boundary layer higher density and the cooling behavior becomes very apparent. Figure 6 heat source parameter Q affects the temperature distribution $\theta(\eta)$, we observed that as the heat source parameter Q decreases, the temperature profile and boundary layer thickness also exhibit a decreasing trend. Figure 7 exhibits that as the chemical reaction parameter S is increased, the fluid temperature $\theta(\eta)$ diminish. Physically, this tendency upwards the sheet temperature $\theta(\eta)$. This phenomenon can be exploited by using fluids with increased chemical reaction properties as coolants. Figure 8 illustrates that as the Lewis number Le is reduced, the concentration profile $\phi(\eta)$ decrease. Physically, this tendency down the, the concentration $\phi(\eta)$. The use of fluids with decreased Lewis number as coolants can capitalize on this effect. Figure 9 reveals the impact of the thermophoresis parameter Nt on the concentration profile $\phi(\eta)$. We see that the distributions of the nanofluids velocity is increase the thermophoresis parameter because are included, indicating that the sheet is pervious. Therefore, as the thermophoresis parameter Nt increases, the thermal boundary layer thickness higher and the cooling behavior becomes very obscure. Figure 10 shows the effect of Brownian motion parameter Nb on concentration profile $\phi(\eta)$. It is observed that the parameters have a decreasing effect on the concentration profile producing a thinner boundary layer. The reason is obvious due to resistive electromagnetic force similar the flow in the primary or main direction. Porosity parameter A on skin friction coefficient $C_{fs}\left(Re_s\right)^{1/2}$ is depicted in Figure 11 the surface drag force of magnitude exhibits a upward trend to increase the value of porosity parameters A. This occurs as decreasing A flattens the surface resulting in increased skin friction coefficient $C_{fs}\left(Re_s\right)^{1/2}$. Viscoelastic coefficient parameter Rc on skin friction coefficient $C_{fs}\left(Re_s\right)^{1/2}$ is depicted in Figure 12 the surface drag force magnitude exhibits a upward trend with rising values of Rc. This is inclining in both Skin friction and heat transfer rate. This occurs because the drag force strengthens with decreasing Viscoelastic coefficient parameter Rc, injecting additional energy into the boundary layer. Porosity parameter A on Nusselt number $Nu_s\left(Re_s\right)^{-1/2}$ is depicted in Figure 13 the surface drag force of magnitude exhibits a downward trend to increase the value of porosity parameters A. This occurs as increasing A flattens the surface resulting in decreased Nusselt number $Nu_s\left(Re_s\right)^{-1/2}$.Viscoelastic coefficient parameter Rc on Nusselt number $Nu_s\left(Re_s\right)^{-1/2}$ is depicted in **Fig.14** the surface drag force magnitude exhibits a upward trend with rising values of Rc. This is inclining in both Nusselt number and heat transfer rate. This occurs because the drag force strengthens with decreasing Viscoelastic coefficient parameter Rc, injecting additional energy into the boundary layer.

The non-linear ordinary differential **Eq.(11), Eq.(12) and Eq.(13)** are solved numerically using MATLAB's bvp4c algorithm, exploring the effect of different values of Magnetic field parameter M, Porosity parameter A, Prandtl number Pr, Darcy Forchheimer Fr, Lewis number Le, Thermophoresis parameter Nt, Brownian motion parameter Nb, Thermal radiation parameter Rd, Heat source parameter Q, Chemical reaction parameter S, Viscoelastic coefficient parameter Rc, Suction parameter b. The numerical results obtained are utilized to illustrate boundary layer profiles of velocity $f'(\eta)$ and temperature $\theta(\eta)$ in the and concentration profile $\phi(\eta)$ form of figures for various values of the relevant parameters. The first step in this approach is to convert the fourth order differential equation into a set of first order equations by defining new variables. It is essential that the assumed solution adheres to the boundary conditions outlined in (14) and reproduce the expected behavior of the solution. Table 1 describes the comparison analysis with the Rajagopal et al.[23] findings. A comparative study is conducted on the skin friction coefficient in terms of $-(1-Rc)f'(0)$ examining the effect of different Viscoelastic parameters.

4 Conclusions

This article focuses on the chemical Reaction effect on MHD viscoelastic nanofluids flow over a stretching sheet embedded in porous media with thermal radiation. The mathematical model includes the Darcy- Forchheimer term in the governing equations for velocity and temperature, enabling the investigation of porous media flows. The Bvp4c solver in MATLAB is utilized to obtain numerical solutions for the nonlinear ordinary differential equations. The main results of this study can be summarized as follows:

- Velocity distributions $f'(\eta)$ rises for increasing values of Magnetic field parameter, Darcy- Forchheimer and while declines for Radiation parameter and Suction parameter.
- In concentration profile $\phi(\eta)$ boosts for higher values of Heat source parameter and declines for Chemical reaction parameter.
- In temperature profile $\theta(\eta)$ boosts for higher values of Lewis number parameter, Brownian motion and declines for Thermophorsis parameter.
- In case of skin friction $C_{fs}\left(Re_s\right)^{1/2}$ shows increasing behavior for Porosity parameter and Viscoelastic parameter
- Nusselt number $Nu_s\left(Re_s\right)^{-1/2}$ increases behavior for Viscoelastic parameter and decline for Porosity parameter.

4.1 Scope and limitations

Scope:

Applicable to industrial processes (heat transfer, materials processing), energy systems (solar collectors, geothermal systems), and biomedical research (drug delivery, tissue engineering), with opportunities for mathematical modeling and numerical analysis.

Limitations:

1. Assumptions of constant fluid properties.
2. Limited to specific geometries (stretching sheet).
3. Neglects certain physical phenomena (e.g., viscous dissipation).
4. Porous media assumptions may not represent all real-world cases.
5. Complexity of nanofluid behavior and chemical reactions.

5 Nomenclature

Fr: Darcy Forchheimer
A: Porosity parameter
M: Magnetic field parameter
Pr: Prandtl number
C_{fs}: Skin friction coefficient
Rc: Viscoelastic coefficient parameter
D_T : Thermophoretic diffusion coefficient
D_B : Brownian diffusion coefficient
$T\infty$: Reference temperature (K)
Tw: Temperature of sheet (K)
Rd: Thermal radiation parameter
q_m: Wall mass flux ($kgm^{-2}s^{-1}$)
q_r: Radiative heat flux (W)
S: Chemical reaction parameter
C_P: Specific heat ($Jkg^{-1}K^{-1}$)
C: Concentration (kgm^{-3})
Re_s : Local Reynolds number
Nu_s : Local Nusselt number
(x, y): Velocity component

b: Suction parameter
a: Positive constant
Nb: Brownian motion
Nt: Thermophoresis parameter
T: Temperature of fluid (K)
C: Concentration of fluid
R: Radius of curvature
k: Mean absorption coefficient
Q: Heat source parameter

Greek symbols:

η : Similarity transformation
$\theta(\eta)$: temperature distribution
$\phi(\eta)$: Concentration distribution
$f'(\eta)$: Velocity distribution
τ : Shear wall stress (Nm^{-2})
$(\rho c)_p$: Ratio of nanoparticles heat capacity
$(\rho c)_f$: Ratio of base fluid heat capacity
σ: Stefan- Boltzmann constant

References

1) Alrehili M. Viscoelastic thermal nanofluid flow and heat mass transfer due to a stretching sheet with slip velocity phenomenon and convective heating. *International Journal of Thermofluids*. 2023 Feb;17:100281. https://doi.org/10.1016/j.ijft.2023.100281.
2) Noor NAM, Shafie S, Admon MA. Impacts of chemical reaction on squeeze flow of MHD Jeffrey fluid in horizontal porous channel with slip condition. *Physica Scripta*. 2021 Jan;96(3):035216. https://doi.org/10.1088/1402-4896/abd821.
3) Hosseinzadeh S, Hosseinzadeh K, Hasibi A, Ganji DD. Hydrothermal analysis on non-Newtonian nanofluid flow of blood through porous vessels. *Proceedings of the Institution of Mechanical Engineers, Part E: Journal of Process Mechanical Engineering*. 2022 Aug;236(4):1604–1615. https://doi.org/10.1177/09544089211069211.
4) Akbari S, Faghiri S, Poureslami P, Hosseinzadeh K, Shafii MB. Analytical solution of non-Fourier heat conduction in a 3-D hollow sphere under time-space varying boundary conditions. *Heliyon*. 2022 Dec;8(12). https://doi.org/10.1016/j.heliyon.2022.e12496.
5) Alrehili M. Development for cooling operations through a model of nanofluid flow with variable heat flux and thermal radiation. *Processes*. 2022 Dec;10(12):2650. https://doi.org/10.3390/pr10122650.
6) Alali E, Megahed AM. MHD dissipative Casson nanofluid liquid film flow due to an unsteady stretching sheet with radiation influence and slip velocity phenomenon. *Nanotechnology Reviews*. 2022 Jan;11(1):463–472. https://doi.org/10.3390/mi13111879.
7) Yousef NS, Megahed AM, Ghoneim NI, Elsafi M, Fares E. Chemical reaction impact on MHD dissipative Casson-Williamson nanofluid flow over a slippery stretching sheet through porous medium. *Alexandria Engineering Journal*. 2022 Dec;61(12):10161–10170. https://doi.org/10.1016/j.aej.2022.03.032.
8) Mahat R, Saqib M, Khan I, Shafie S, Noor NA. Thermal radiation effect on Viscoelastic Walters'-B nanofluid flow through a circular cylinder in convective and constant heat flux. *Case Studies in Thermal Engineering*. 2022 Nov;39:102394. https://doi.org/10.1016/j.csite.2022.102394.
9) Afridi MI, Chen ZM, Riaz N, Qasim M. Impact of porous and magnetic dissipation on dissipative fluid flow and heat transfer in the presence of Darcy-brinkman porous medium. *Journal of Porous Media*. 2024;27(3). https://doi.org/10.1615/JPorMedia.2023045345.
10) Kavitha R, Pasupulla AP, Panneerselvam P. Numerical Investigation on Heat and Mass transfer through a porous medium in the presence of MHD and Chemical Reaction. *Turkish Journal of Computer and Mathematics Education*. 2021;12(2):1178–1182. Available from: https://turcomat.org/index.php/turkbilmat/article/view/1140.
11) Roja P, Ibrahim SM, Reddy TS, Lorenzini G. Chemically Radiative MHD Flow of a Micropolar Nanofluid over a Stretching/Shrinking Sheet with a Heat Source or Sink. *Fluid Dynamics & Materials Processing*. 2024 Feb;20(2). https://doi.org/10.32604/fdmp.2023.042283.
12) Saleh S, Saad N, Emmanuel O. Magnetohydrodynamic (MHD) Convective Flow through a Porous Medium with Magnetic and Chemical Reaction Characteristics. *International Journal of Science for Global Sustainability (IJSGS)*. 2024 Mar;10(1). https://doi.org/10.57233/ijsgs.v10i1.591.
13) Sandhya A, Reddy GVR, Deekshitulu VS. Heat and mass transfer effects on MHD flow past an inclined porous plate in the presence of chemical reaction. *International Journal of Applied Mechanics and Engineering*. 2020;25(3). https://doi.org/10.2478/ijame-2020-0036.
14) Jothimani S. Unsteady Casson fluid flow past a stretching sheet with radiation absorption and chemical reaction. *JP Journal of Heat and Mass Transfer*. 2024 Jan;37(1):67–86. https://doi.org/10.17654/0973576324005.
15) Hosseinzadeh S, Hosseinzadeh K, Hasibi A, Ganji DD. Hydrothermal analysis on non-Newtonian nanofluid flow of blood through porous vessels. *Proceedings of the Institution of Mechanical Engineers, Part E: Journal of Process Mechanical Engineering*. 2022 Aug;236(4):1604–1615. https://doi.org/10.1177/09544089211069211.
16) Mukhtar S, Rana S, Mansoor M, Arooj T, Hassan QMU, Shah R. MHD viscoelastic nanofluid flow across an extended plate using mixed convection and thermal radiation. *Frontiers in Energy Research*. 2024 Mar;12:1275652. https://doi.org/10.3389/fenrg.2024.1275652.
17) Hymavathi D. Micropolar Nanofluid Flow, Thermal and Mass Transfer Properties Across a Stretching Sheet With a Predetermined Surface Heat Flux. *Communications in Mathematics and Applications*. 2023;14(2):619.
18) Reddy MV, Nath JM, Das TK, Ali F, Shah NA. Mixed convection flow on the Hall current effect of Ree-Eyring nanomaterial with gyrotactic microorganism and heat radiation flow. *Journal of Thermal Analysis and Calorimetry*. 2025 Apr. https://doi.org/10.1007/s10973-025-14093-z.
19) Devika B, Prasad MK, Venkateswarlu B, Bahajjaj AA. Exploring the significance of nanoparticle shapes and the impact of thermal radiation on MHD viscoelastic nanofluid flow in porous channels. *International Journal of Modelling and Simulation*. 2024 Sep. https://doi.org/10.1080/02286203.2024.2392219.

20) Anwar MS, Khan M, Hussain Z, Muhammad T, Puneeth V. Investigation of heat transfer characteristics in MHD hybrid nanofluids with variable viscosity and thermal radiations. *Journal of Radiation Research and Applied Sciences*. 2025 Mar;18(1):101240. https://doi.org/10.1016/j.jrras.2024.101240.
21) Ahmed WA, Onyango ER, Theuri D, Awad F. Heat and Mass Transfer on MHD Nanofluid Flow with Temperature-dependent Viscosity in the Presence of Chemical Reaction. *American Journal of Nano Research and Applications*. 2024;12(2):29–44. https://doi.org/10.11648/j.nano.20241202.12.
22) Rashidi MM, Ali M, Rostami B, Rostami P, Xie GN. Heat and mass transfer for MHD viscoelastic fluid flow over a vertical stretching sheet with considering Soret and Dufour effects. *Mathematical Problems in Engineering*. 2015;2015:861065. https://doi.org/10.1155/2015/861065.
23) Rajagopal KR, Na TY, Gupta AS. Flow of a viscoelastic fluid over a stretching sheet. *Rheologica Acta*. 1984 Mar;23:213–215. http://dx.doi.org/10.1007/BF01332078.